



CHALMERS
UNIVERSITY OF TECHNOLOGY

Solvent extraction of cobalt from spent lithium-ion batteries: Dynamic optimization of the number of extraction stages using factorial design of

Downloaded from: <https://research.chalmers.se>, 2024-04-27 01:33 UTC

Citation for the original published paper (version of record):

Vieceli, N., Ottink, T., Stopic, S. et al (2023). Solvent extraction of cobalt from spent lithium-ion batteries: Dynamic optimization of the number of extraction stages using factorial design of experiments and response surface methodology. *Separation and Purification Technology*, 307.
<http://dx.doi.org/10.1016/j.seppur.2022.122793>

N.B. When citing this work, cite the original published paper.



Solvent extraction of cobalt from spent lithium-ion batteries: Dynamic optimization of the number of extraction stages using factorial design of experiments and response surface methodology

Nathália Vieceli^{a,*}, Thomas Ottink^a, Srečko Stopić^b, Christian Dertmann^b, Thomas Swiontek^c, Claudia Vonderstein^b, Reiner Sojka^c, Niclas Reinhardt^d, Christian Ekberg^a, Bernd Friedrich^b, Martina Petranikova^a

^a Department of Chemistry and Chemical Engineering, Industrial Materials Recycling and Nuclear Chemistry, Chalmers University of Technology, Chalmers University of Technology, SE-41296 Gothenburg, Sweden

^b IME – Process Metallurgy and Metal Recycling, Institute and chair at RWTH Aachen University, Intzestr. 3, 52056 Aachen, Germany

^c Accurec-Recycling GmbH, Bataverstr. 21, DE 47809 Krefeld, Germany

^d MEAB Metallextraktion AB, Datavägen 51, S-436 32 Askim, 2, Sweden

ARTICLE INFO

Keywords:

Solvent extraction
Recycling
Cobalt
Lithium-ion batteries
Cyanex 272

ABSTRACT

The optimization of lithium-ion batteries (LiBs) recycling is crucial not only from a waste management perspective but also to decrease the dependence on imports of critical raw materials. In addition, the diversification of the recycling technologies is very important for better flexibility of the market. This study aims at investigating the recovery of Co from spent LiBs using solvent extraction from a real chloride-based solution obtained after the removal of Mn, which is very rarely reported. Cyanex 272 was used as the extractant and the effect of several variables on the extraction efficiency was considered to model and optimize the separation of Co and Ni. The number of extraction stages directly affects not only the process efficiency but also its cost. Thus, in this work, a novel approach was developed to assist in the selection of the number of extraction stages using a dynamic method based on the factorial design of experiments and response surface methodology combined with the Kremser's Equation. This method can assist the process design, decrease the overall cost of the operation, and optimize the separation of Co and Ni in a reduced number of extraction stages. The concentration of Co and Ni in the feed solutions is ~ 8.3 g/L and 1.9 g/L, respectively. Based on the results, 98% extraction efficiency for Co can be achieved in 1 to 2 extraction stages with low co-extraction of Ni (<5%) when using 0.6–0.8 M Cyanex 272, O:A ratio below 1 and pH ~ 5, but several combinations of conditions could provide similar results.

1. Introduction

Lithium-ion batteries (LiBs) are key in the transition to a fossil-fuel-free society and their use in electric vehicles (EVs) and stationary energy storage has grown exponentially in the last years [1]. In 2021, EV sales reached a new record of 6.6 million and nearly 10% of global car sales were electric, which represents four times the market share in 2019 [2]. This increasing trend is expected to continue boosting the LiBs battery market, which is projected to grow 30% per year until 2030, mainly driven by electric vehicles [3,4].

With the increasing demand for LiBs, the supply risk of raw materials creates an additional challenge to developing high-density, low-cost

batteries for EVs [5]. Cobalt (Co) has been recognized as an essential element for LiB cathode chemistry and it has been used from the first cathode commercialized (LiCoO₂) in 1991 to the present Li[Ni_xCo_y(Mn or Al)_{1-x-y}]O₂ [5], offering high conductivity and stable structural stability throughout charge cycling [6]. Co can account for 20% of the weight of the cathode in EV LiBs [7] and it is considered the highest material supply chain risk for EVs in the short and medium-term [7].

Cobalt is produced mainly as a by-product or co-product of Ni and Cu and for this reason, its supply is not independent of other commodity businesses [8–7]. Additionally, mining and refining of Co involve environmental and social concerns [5] – in 2018, ~60% of the worldwide mine production of Co originated from Cu-Co ores in the Democratic

* Corresponding author.

E-mail address: nathalia.vieceli@chalmers.se (N. Vieceli).

<https://doi.org/10.1016/j.seppur.2022.122793>

Received 1 September 2022; Received in revised form 23 November 2022; Accepted 25 November 2022

Available online 28 November 2022

1383-5866/© 2022 The Authors. Published by Elsevier B.V. This is an open access article under the CC BY license (<http://creativecommons.org/licenses/by/4.0/>).

Republic of the Congo, where geopolitical instability and unethical working conditions are well documented and can impact the Co exports [9]. Consequently, given its strategic importance associated with supply risks, Co is present in the list of critical raw materials for the European Union since it was first published in 2011 [10] and it is also classified as a critical resource for the United States [11]. In addition, there has been a strong pressure to reduce Co from current cathode materials, motivated by economic, environmental, security, and societal drivers [5–7]. Even though the battery makers continue to move to lower Co content chemistries (and even Co-free chemistries by 2030), the rise in global demand for EV batteries still increases the total Co demand this decade [2]. In this context, sustainable recovery of metals from spent LIBs may be of great significance regarding the conservation of metal resources [12] and closed-loop recycling can help create additional supply and alleviate the demand for primary resources [13] and its impacts.

An overview of the recovery of Co from spent LIBs was recently published by Mansur *et al.* [14]. Among the main recycling methods for spent LIBs (pyrometallurgy, hydrometallurgy and a combination of both), the hydrometallurgical approach has attracted increasing attention and is currently the mainstream method for laboratory research and industrial application [12–15]. Additionally, transition metal separation using solvent extraction is generally needed after pyrometallurgical processing. Thus, there is no possibility to avoid using hydrometallurgy in LIBs recycling. However, the leaching liquors obtained from spent LIBs are complex and contain not only Co ions, but also Ni, Mn, Cu, and other metal ions. For this reason, it is difficult to obtain pure Co compounds from these solutions, given the similar physicochemical properties of these metals [16]. Traditionally, Co and Ni have been separated by selective oxidation and/or precipitation of Co. However, unlike the precipitation processes, solvent extraction provides the opportunity for better Co/Ni separation, with high yields and purity of the separated metals [17,18].

When it comes to solvent extraction extractants, the separation ability of Co and Ni increases in the order of phosphinic > phosphonic > phosphoric acid, which can be attributed to the increasing stabilization of tetrahedral coordination of cobalt complexes with the extractant in the organic phase, since the tetrahedral compound is more stable than the octahedral one [19]. Thus, commercial extractants like Cyanex 272, D2EPHA and PC 88A should primarily be used depending on the solution composition [20]. Cyanex 272 offers some advantages over the alternative organophosphorus extractants, including high Ni/Co selectivity, the ability to reject Ca [21], and it allows the solvent extraction of Co from liquors containing very different ratios of cobalt and nickel [22]. According to Flett [22], by 2005, there were 13 plants located in Western Europe, South America, Canada, Africa, China, and Australia using Cyanex 272 for Co separation and recovery from Ni, and the extractant was used to produce ~ 50% of Co in the Western world. However, an issue in Co extraction is the stability of the organic phase. Co²⁺ + ion can act as a catalyst to oxidize hydrocarbon diluents to carboxylic acids, which would reverse the Co/Ni selectivity obtained with Cyanex 272. A standard practice to improve diluent stability is using phenolic oxidation inhibitors, such as BHT (butylhydroxytoluene), to prevent carboxylic acid formation, maintain cobalt–nickel selectivity and facilitate normal plant operations [22,23].

The selective removal of Co from leachates from spent LIBs using solvent extraction has been widely investigated and the main results of some of these studies are presented in Table 1. However, process optimization is usually performed by varying one variable at a time, without evaluating the interaction effects of process variables. In this context, the main goal of this study was to implement an improved method to optimize the solvent extraction of Co and its separation from Ni using factorial design of experiments and response surface methodology to evaluate the interaction effect of different variables on the operation. The tests were carried out using Cyanex 272 as the extractant and a chloride-based raffinate, which is another innovative aspect of this work considering that chloride-media has been very rarely investigated when

Table 1
Summary of conditions from published studies on the solvent extraction of Co from LIB solutions (best conditions reported).

Extractant	Saponification	Modifier	O:A	Optimum pH	Temperature (°C)	Contact time (min)	Feed	Initial composition (g/L)				Efficiency (%)		Ref.
								Mn	Co	Ni	Li	Co	Ni	
0.4 M Cyanex 272	50% (with NaOH)	no	2:1	6	room	30	Leachate from spent LIBs. Leaching with H ₂ SO ₄ and precipitation of Cu, Fe and Al with NaOH.	<0.1	13.8	<0.1	2	95–98	~1	[24]
0.4–0.5 M Cyanex 272	no	no	1:1	6–7	22	12	Spent batteries leached with sulfuric acid and hydrogen peroxide.	–	12	–	–	97–99	–	[25]
0.1 M Cyanex 301	no	no	1:1	7.2	25–55	15	Synthetic leachate based on spent LIBs using chloride media.	–	1	0.1	0.3	99	15	[26]
30% vol. PC-88A	30% (with NaOH)	5% v/v TBP	1:1	4.2	room	10	Spent LIBs leached with sulfuric acid and H ₂ SO ₄ . Previous SX for Cu and Mn using D2HPA.	–	> 8	–	–	80	–	[16]
1.5 M Cyanex 272	65% (with NaOH)	5% v/v TBP	1.6:1	5–5.3	25	10	Waste LCO from process manufacturing. Leaching with H ₂ SO ₄ and H ₂ O ₂ .	–	44.7	–	5.4	85–99	–	[27]
25% w/w P507	70% (with NaOH)	TBP	1.5:1	4.1	25	10	LIBs from phones after thermal treatment and removal of foils. Leaching with H ₂ SO ₄ and H ₂ O ₂ and precipitation of impurities.	≤0.1	20	0.5	2.5	95	< 5	[28]
0.72 M Cyanex 272	no	no	1:1	5	50	20	LIBs (LCO) after leaching with H ₂ SO ₄ and H ₂ O ₂ and removal of impurities with NH ₄ OH.	–	10.7	–	0.9	88	–	[29]
0.56 M PC-88A	~60 (with NaOH)	no	3:1	4.5	25	10	Cathode scrap leached with H ₂ SO ₄ and H ₂ O ₂ , followed by oxidative precipitation of Mn and SX with D2EHPA (Mn, Al, Fe removal).	–	25.1	2.5	6.2	>99	4.3	[30]

compared to sulfate media solutions but could allow the reuse of hydrochloric acid recovered from different processes and also to decrease the consumption of NaOH. The raffinate was obtained after the removal of Mn by solvent extraction with D2EHPA from a leachate produced from spent LIBs. Additionally, an novel method to optimize the number of extraction stages to reach 98% Co extraction efficiency and estimate the co-extraction of Ni under varied operational conditions was developed in this study. For this, the measured Co and Ni concentrations were used to fit regression models predicting concentration of Co and Ni depending on the process conditions, which were then used to perform a dynamic optimization of the number of extraction stages using the Kremser's equation. This approach can help to improve the process design, decreasing costs and improving its resource efficiency.

2. Materials and methods

2.1. Sample preparation: Solid samples and physical processing

The physical processing of the battery packs was performed by Accurec Recycling GmbH (Germany). Battery packs from different sources and chemistries were discharged in a vacuum chamber and then mechanically treated using an impact mill, liberating the cells from their casing. The cells were subjected to pyrolysis using an electrically heated, stainless-steel retort with an attached subsequent condensing system and redundant evacuation equipment. The electrolyte was distilled during the process by incremental heating and organic components present in the separator and binder were pyrolyzed. The outcome fraction was submitted to shredding and magnetic separation of the Fe-rich fraction and steel casing. The resultant material was sieved, and the fine fraction (<1 mm) was used in the hydrometallurgical route.

2.2. Sample preparation: leaching, purification, and removal of Mn

The leachate used in this study was produced by the Institute IME Process Metallurgy and Metal Recycling (RWTH Aachen University, Germany) through the acid leaching of the black mass (fine fraction, < 1 mm) using 4 M HCl, 50 g/L H₂O₂ (35%), solid to liquid ratio of 100 g/L, 300 rpm, 120 min at 80 °C. The leachate was purified by cementation with Fe to remove Cu, followed by precipitation with NaOH (5 M) to remove Al and Fe. After that, the pH was increased to ~ 10 using NaOH and Ni, Co, and Mn were precipitated as a mixture of hydroxides. Leaching, cementation, and purification were carried out as batch reactions. The mixture of hydroxides was sent to the Industrial Materials Recycling group (Chalmers University of Technology, Sweden) as a pulp, which was redissolved in 0.5 M HCl (4.20 g/L Mn, 13.3 g/L Co, 2.8 g/L Ni). Mn was then removed from this solution by solvent extraction in mixer-settlers operating in counter-current (aqueous phase and organic phase flow in opposite directions in the mixer-settlers) at the following conditions: 2 extraction stages using 0.5 M D2EHPA (di-(2-ethylhexyl) phosphoric acid, diluted in Isopar L), organic to aqueous ratio (O:A) of 1:1 and equilibrium pH of 2.3; 1 scrubbing stage using 4 g/L Mn (MnCl₂·4H₂O), O:A 1:1; 1 stripping stage using 0.5 M HCl, O:A 1:1. The flow rate for all the streams was constant (5 mL/min, volume of the mixer-chamber 30 mL, volume of the settling area 120 mL, residence time in the mixing chamber ~ 6 min). The extraction efficiency of Mn was 96%, while around 18% Co, 15% Li and 13% Ni were co-extracted in two stages but could be quantitatively removed from the loaded organic by scrubbing. The concentration of the final raffinate is presented in Table 2 and it was used in the solvent extraction experiments to separate Co from Ni.

2.3. Preparation of the organic phase

Bis(2,4,4-trimethylpentyl) phosphinic acid (commercially available as Cyanex 272, Cytec) was used as the extractant as it was supplied, without any additional purification, and Isopar L (high purity synthetic

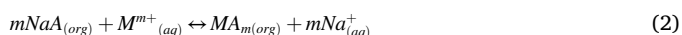
Table 2

Concentration in the raffinate after solvent extraction of Mn with D2EHPA in mixer-settlers.

Element	Concentration (mg/L)	Element	Concentration (mg/L)
Co	8318	Cu	100
Ni	1947	Mg	9
Li	900	Al	< LOD*
Mn	143	Zn	< LOD*

*LOD: limit of detection.

isoparaffinic hydrocarbon fluid, C11-C13. <2% aromatics, ExxonMobil Chemical [31,32]) was used as the diluent. The extractant was saponified to start extraction experiments closer to the pH range of interest and to make it easier to adjust the pH. The saponification can be described according to Eq. (1), while the extraction mechanism with the saponified extractant can be represented by Eq. (2) [33].



where *HA* represents the extractant, *M^{m+}* represents the metal cations, and *MA_{m(org)}* the complex formed. In the extraction process, no *H⁺* is released and higher equilibrium pH can be held, which promotes higher extraction efficiency [33].

Extractant solutions with different saponification rates were used and were prepared by adding stoichiometric amounts of 10 M NaOH. The saponification was performed in sealed plastic cups (100 mL) while heating with a water bath and mixing with a magnetic stirrer at 500 rpm. Isopar and NaOH were added to the cup and were preheated to 50 °C. Cyanex 272 at 50 °C was then added to the cup and the solution was left to react for 1 h at the same temperature and stirring speed.

2.4. Experimental setup and preliminary experiments

Preliminary extraction tests investigating the effects of contact time and saponification ratio were performed in glass vials (3.5 mL) at room temperature using an O:A of 1:1. A shaking machine (IKA, VXR basic Vibrax®) operating at 1000 vibrations per minute was used to promote contact between phases. After a set time limit, the phases were separated by centrifugation (Frontier™ 5000 series, OHAUS) at 5000 rpm for 5 min. The pH of the aqueous phase was measured using a pH electrode (905 Titrand, Metrohm) which was regularly calibrated before the experimental procedures. Samples were taken from the aqueous phase and were diluted with 0.5 M HNO₃ (ultrapure grade, 69–70%, Sigma Aldrich) to analyze their chemical composition with Inductively Coupled Plasma – Optical Emission Spectroscopy (ICP – OES, iCAP™ PRO XP, ThermoFisher).

Further preliminary tests studying the effects of pH, the concentration of Cyanex 272, organic to aqueous ratio (O:A) and addition of 5% tributyl phosphate (TBP) as a modifier in the organic phase, were performed in plastic containers (100 mL). A stirrer from mixer-settler equipment operating at 1000 rpm was coupled to the plastic containers and used for contacting phases. All tests were performed at room temperature using a total volume of 30 mL. This setup was also used in the optimization of the extraction process as described in section 2.3. Extractant solutions were 20% saponified and the pH was thereafter adjusted by the dropwise addition of 10 M NaOH or 5 M HCl to the system followed by 15 min of stirring. After contacting, phases were left to separate for at least 10 min and the pH of an aqueous phase sample was measured.

When the pH reached a desired level, a sample was taken from the aqueous phase, diluted with 0.5 M HNO₃ (ultrapure grade, 69–70%, Sigma Aldrich) and analyzed with ICP – OES. The elemental composition of the organic phase was determined by mass balance, considering the initial elemental composition of the solution shown in Table 2 (raffinate

after the removal of Mn) and the final concentrations measured by ICP – OES in the raffinate. The extraction efficiency for different elements was determined using Eq. (3).

$$E(\%) = 100 \times \frac{D_X}{D_X + V_{aq}/V_{org}} \quad (3)$$

where V_{aq} and V_{org} are volumes of the aqueous and organic phase respectively. The distribution factor D_X was also used to get an understanding of the extraction behavior of different elements and can be calculated using Eq. (4)

$$D_X = \frac{C_{X,org}}{C_{X,aq}} \quad (4)$$

where $C_{X,org}$ and $C_{X,aq}$ are concentrations of element X in the organic and aqueous phase respectively. To quantify the degree of separation between two analytes (X and Y), the separation factor β in Eq. (5) can also be used.

$$\beta = \frac{D_X}{D_Y} \quad (5)$$

2.5. Optimization using factorial design of experiments

Optimization of the extraction process was accomplished using the design of experiments and response surface methodology. Factorial design is a useful technique to investigate main and interaction effects of variables chosen in a design of experiment, being helpful to investigate the interaction effects of independent variables on the process outputs (dependent variables) [34]. The values experimentally obtained through different combinations of factors are statistically analyzed and the process response obtained for a combination of factor levels is represented by a function. It is assumed that the responses can be predicted by low-order polynomial functions of the independent variables, which are determined as a particular case of multiple linear regression [35–37]. A detailed explanation of these methods is given by Montgomery [38]. An inscribed central composite design (CCD) with $\alpha = 0.59$ was used to optimize the separation of Co and Ni and avoid extreme conditions in the highest factor levels. The experimental error was estimated with 4 replicates of the center point experiment. All experiments were performed in random order. The effects of three factors on responses were investigated: organic to aqueous ratio (x_1), pH (x_2) and concentration of Cyanex 272 (x_3). The factor levels are shown in Table 3 and were selected based on results from preliminary tests and literature review.

Measured concentrations of Co, Ni, Mn, Cu and Li in the raffinate were used to calculate extraction efficiencies for each metal using Eq. (3), which were used as process responses (Y). Efficiencies for Co and Ni were used to fit linear second-order regression models with interaction terms using the least squares method. Regression terms were tested on a 95% confidence basis by comparing standardized effects of regression coefficients against a t -distribution. Only significant terms were included in the regression model. Analysis of variance (ANOVA) was used to determine the significance of regression models and test for lack of fit (95% confidence basis). The coefficient of determination (R^2) was

used to evaluate the goodness of fit of each model. Response surfaces and contour plots were used to visualize the results from the fitted models for Co and Ni and aid in the optimization of extraction conditions.

2.6. Dynamic optimization of the number of extraction stages

The concentrations of Co and Ni measured in the raffinate in the factorial design were used to perform a dynamic optimization of the number of extraction stages required to achieve an extraction efficiency of 98% Co. For this, these concentrations were used to also fit regression models predicting the concentration of Co and Ni in the raffinate depending on the process conditions. From these models and knowing the initial concentration of Co and Ni in the feed solution (Table 2), the estimated concentrations of Ni and Co in the loaded organic were calculated by mass balance. The results were used as input for Kremser's equation (Eq. (6)) to predict the number of extraction stages theoretically needed to reach 98% extraction efficiency for Co under several combinations of process conditions and to estimate the resulting co-extraction of Ni.

$$\phi = \frac{(P - 1)}{(Pn + 1 - 1)} \quad (6)$$

Where ϕ is the non-extracted fraction and P is the extraction factor that can be calculated using Eq. (7).

$$P = D \times \Theta \quad (7)$$

Where D is the distribution factor and Θ is the phase ratio that represents the ratio between the volume of organic phase (V_{org}) and the volume of aqueous phase (V_{aq}). When $P \leq 1$, Eq. (8) was considered to relate the process efficiency to the number of extraction stages.

$$\phi = \frac{1}{(n + 1)} \quad (8)$$

3. Results and discussion

3.1. Preliminary tests: Effect of contact time and saponification rate

The effect of the contact time on the extraction efficiency of different metals was evaluated using different saponification levels (Fig. 1). The extraction of Li was in general low (<15%) and the results were omitted from the graphs. Magnesium had low extraction efficiencies (<25%) and since it is present in a very low concentration in the feed solution, its behavior was also not followed. For Co, the extraction efficiency was not stable after 10 and stabilized after 15 min of contact time and for this reason, the contact time was set at 15 min in the next experiments. The average pH for different saponification levels was 10% = 3.6, 20% = 3.9, 30% = 4.2, 40% = 4.5, 50% = 5.5 and 60% = 5.6 (standard deviation ± 0.1). Based on these results, to have a better control of pH and study its effects on the extraction, it was decided to set the saponification rate at 20% in the following preliminary tests.

3.2. Preliminary tests: Effect of extractant concentration on efficiency

The effect of different concentrations of Cyanex 272 on the extraction efficiency at different pH is shown in Fig. 2. Increasing concentrations of extractant and pH promoted an increase in the extraction efficiency. As expected, Co, Cu and Mn had similar behavior, however, the concentration of Co in the feed solution was much higher (>8 g/L Co) than the other metals (~100 mg/L Cu and Mn). Cyanex 272 had a better selectivity towards Co/Ni and the extraction efficiency of Ni (~2 g/L in the feed) remained low at pH below 5.5 and then started to increase with the increase of pH. The extraction efficiency of Li remained low (<8%) and it was not represented in these graphs (see Fig. 3).

Table 3
Factorial levels used in the experimental design.

Factors	Coded variable	Levels		
		Low (-1)	Standard (0)	High (+1)
Organic to aqueous ratio (O:A, dimensionless)	x_1	1:2	1:1	2:1
Equilibrium pH (dimensionless)	x_2	4	5	6
Concentration of Cyanex 272 (M)	x_3	0.4	0.6	0.8

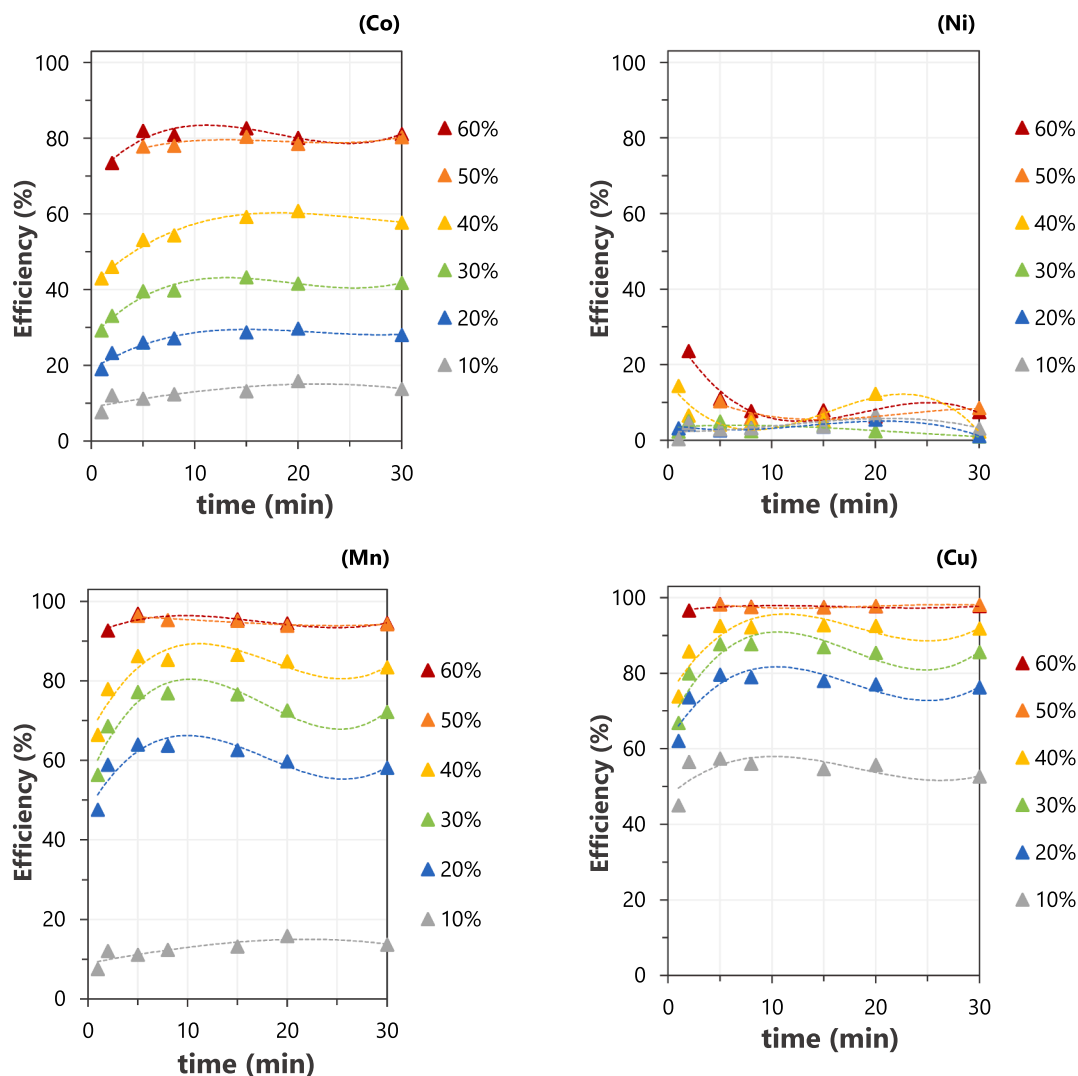


Fig. 1. Extraction efficiencies at different contact times and saponification ratios. Conditions: 0.4 M Cyanex 272 and O:A of 1:1, contact time: 1, 2, 5, 8, 15, 20 and 30 min.

Increasing the pH above 6 is not recommended and can cause precipitation of cobalt hydroxide and third phase formation, which is related to the high viscosity of the organic phase [30]. Moreover, according to Devi *et al.* [39] Cyanex 272 extraction systems should be operated at a maximum of 60% of the loading capacity, to prevent a large increase in viscosity and consequent decrease in the mass transfer rate. Although precipitation was not observed in the experiments at pH above 6, possibly because the extraction reaction is fast, an increase in the viscosity of the loaded organic was visually observed with the increase in the pH, where loading of the extractant was high. Therefore, the pH was limited to 6 in the factorial design of experiments and the same range of concentrations of extractant as in the preliminary experiments was tested.

3.3. Preliminary tests: Effect of organic to aqueous ratio on efficiency

Increasing the O:A ratio led to an increase in the extraction of Co, Ni, and Li, which is expectable since it represents higher availability of extractant to react with (Fig. 3). Cu and Mn are not represented in the graphs and were fully extracted at pH above 5, regardless of the O:A ratio. Lowering the equilibrium pH could increase the selectivity of the extractant towards Co even when using a higher O:A ratio and therefore, the O:A 2:1 was selected as the highest level to be tested in the design of

experiments (DOE) for this variable. However, it is important to mention that a high O:A ratio decreases the concentration of the target metal in the loaded organic and the purity, and for this reason, lowering the O:A ratio to 1:2 was also evaluated in the DOE.

3.4. Preliminary tests: Effect of the use of modifier

TBP (tributyl phosphate) is commonly used as a modifier in the solvent extraction of Co and it was employed in some of the studies reported in Table 1. The role of a modifier is to prevent the third phase formation, but the extractive properties can also be affected by modifiers [40]. In this work, the effect of adding 5% v/v TBP (Sigma-Aldrich, $\geq 99\%$) in the organic phase was compared to the absence of the modifier and the results are presented in Fig. 4. The addition of 5% v/v TBP did not promote a relevant increase in the extraction of Co, Mn, or Cu. A slight increase in the extraction of Li was observed. An increase in the extraction of Ni was verified at pH levels up to 5.5, which could negatively affect the separation of Co and Ni. Additionally, since no problems with phase separation were observed, it was decided to not use TBP in the subsequent experiments.

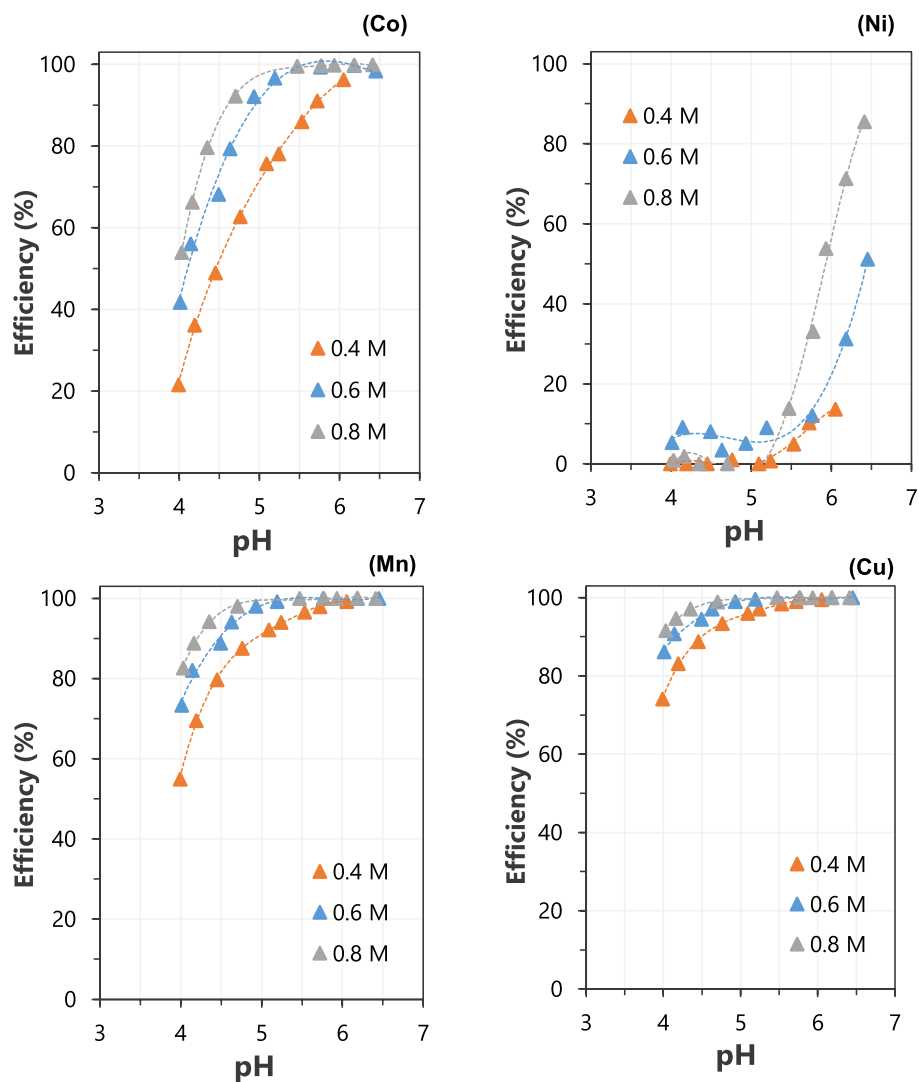


Fig. 2. Extraction efficiencies of metals at different pH levels using different molar concentrations of Cyanex 272 (0.4 M, 0.6 M and 0.8 M). Conditions: 15 min contacting time, O:A of 1:1 and 20% saponified Cyanex 272.

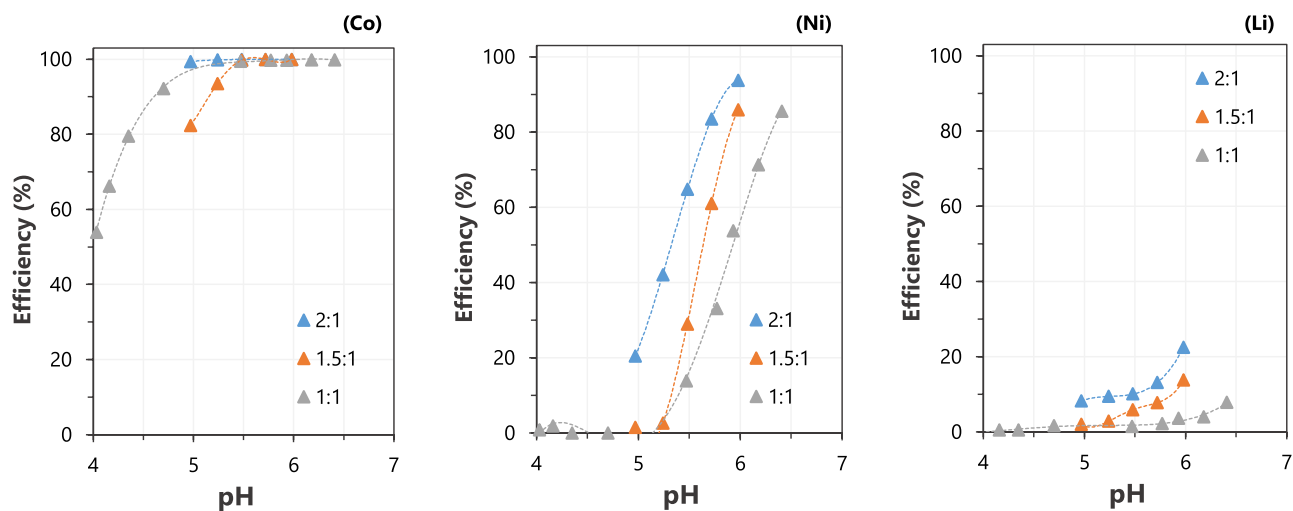


Fig. 3. Extraction efficiencies of metals at different pH levels and O:A ratios. Conditions: 15 min contacting time and 0.8 M Cyanex 272 saponified at 20%.

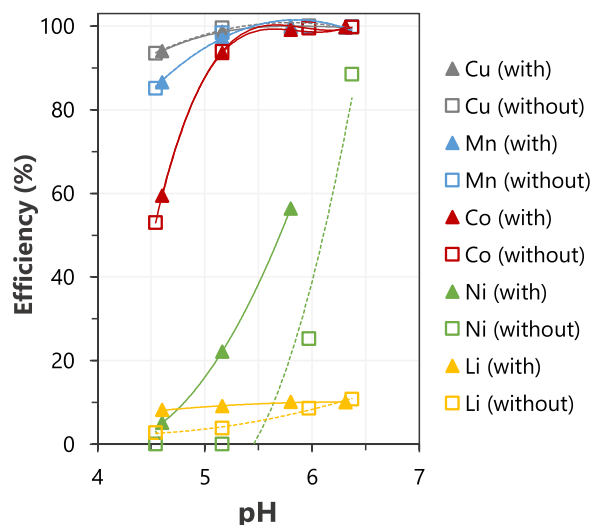


Fig. 4. Extraction efficiencies of metals at different pH levels with 5% v/v TBP and without TBP in the organic phase. Conditions: 15 min contacting time, O:A of 1:1 and, 0.8 M Cyanex 272 saponified at 20%.

3.5. Factorial design of experiments and regression models

The experimental conditions considered in the factorial design of experiments are presented in Table 4 along with the correspondent extraction efficiencies for different metal ions (responses) and the final concentrations measured in the raffinate for Co and Ni. Experiments 9 to 12 in the standard order correspond to replicates in the central point of the design.

The regression models for Co and Ni extraction efficiency are represented by Eqs. (9) and (10), respectively.

$$\begin{aligned} Co(\%) = & 93.0 + 19.4x_1 + 23.7x_2 + 13.1x_3 - 12.2x_1x_2 - 10.6x_1x_3 - 11.4x_1^2 \\ & - 20.5x_2^2 - 7.3x_3^2 \end{aligned} \quad (9)$$

$$\begin{aligned} Ni(\%) = & 10.1 + 10.8x_1 + 8.5x_2 + 6.9x_3 + 15.9x_1x_2 + 15.8x_1x_3 + 14.3x_2x_3 \\ & + 23.9x_1x_2x_3 \end{aligned} \quad (10)$$

Table 4

Experimental conditions for the inscribed central composite design (CCI) with extraction efficiency responses for Co, Ni, Mn, Cu and Li and concentrations in the raffinate for Co and Ni. Conditions: 15 min contacting time and 10% saponified Cyanex 272.

Random Order	Standard Order	Coded Variables			Real Variables			Response (Efficiency, %)					Response (Concentration, mg/L)*	
		x_1	x_2	x_3	O:A	pH	Cyanex 272 (M)	Co	Ni	Mn	Cu	Li	Co	Ni
17	1	-0.59	-0.59	-0.59	1.5:1	4.4	0.48	40	2	74	85	1	4961	1917
16	2	0.59	-0.59	-0.59	1:1.5	4.4	0.48	76	6	93	96	5	2000	1831
15	3	-0.59	0.59	-0.59	1.5:1	5.6	0.48	72	2	92	97	1	2289	1911
2	4	0.59	0.59	-0.59	1:1.5	5.6	0.48	99	9	100	100	1	39	1778
1	5	-0.59	-0.59	0.59	1.5:1	4.4	0.72	62	3	87	93	4	3120	1878
5	6	0.59	-0.59	0.59	1:1.5	4.4	0.72	92	10	98	99	10	674	1748
8	7	-0.59	0.59	0.59	1.5:1	5.6	0.72	96	4	99	99	2	292	1871
6	8	0.59	0.59	0.59	1:1.5	5.6	0.72	100	53	100	100	8	9	912
7	9	0	0	0	1:1	5	0.6	92	2	98	99	2	638	1905
9	10	0	0	0	1:1	5	0.6	93	15	98	99	13	545	1654
13	11	0	0	0	1:1	5	0.6	93	8	98	99	7	546	1795
10	12	0	0	0	1:1	5	0.6	93	7	98	99	7	557	1801
3	13	-1	0	0	1:2	5	0.6	62	5	88	94	5	3161	1854
18	14	1	0	0	2:1	5	0.6	99	17	99	100	10	74	1617
4	15	0	-1	0	1:1	4	0.6	43	4	75	87	4	4712	1860
11	16	0	1	0	1:1	6	0.6	100	18	100	100	6	27	1600
12	17	0	0	-1	1:1	5	0.4	72	7	91	95	7	2366	1810
14	18	0	0	1	1:1	5	0.8	98	9	99	99	7	187	1769

* Concentration measured in the raffinate (aqueous phase).

Table 5

ANOVA table for regression models for Co and Ni extraction efficiencies.

Response	Source	Sum of squares	Degrees of freedom	Mean square	F-value	Critical F-value
Co	Regression	6442.2	10	644.2	54.64	3.64
	Residual	82.5	7	11.8	–	–
	Lack of fit	81.7	4	20.4	71.54	9.12
	Pure error	0.9	3	0.3	–	–
	Total	6524.7	17	–	–	–
Ni	Regression	2048.3	7	292.6	9.01	3.14
	Residual	324.9	10	32.5	–	–
	Lack of fit	240.7	7	34.4	1.23	8.89
	Pure error	84.2	3	28.1	–	–
	Total	2373.2	17	–	–	–

All quadratic terms were eliminated from the model for Ni to improve the goodness of fit (R^2). The analysis of variance (ANOVA) for the fitted models is presented in Table 5. The Residual Sum of Squares was decomposed into the Sum of Squares due to Pure Error (estimated from the replicates in the central level) and the Sum of Squares due to Lack of Fit. The results of the F-tests are significant and the results of the Lack of Fit test also indicate the adequacy of the adjusted models (p-value > 0.05).

It is possible to observe from the coefficients of determination (R^2 , Fig. 5) that the model for Co has a better fit to the experimental data. The standardized effects of different factors on the responses for Ni and Co efficiency are presented as horizontal bars in Fig. 6 and are more significant the more to the right of the dashed red line they are (0.975 quantile of the Student's t -distribution depending on the degrees of freedom).

3.6. Response surfaces for the extraction of Co and Ni

Contour plots representing the response surfaces were constructed based on the fitted models using a pair of variables (x_1 = organic to aqueous ratio and x_2 = pH) varying from the low to the high level and keeping a third factor constant (x_3 = concentration of Cyanex 272). The contour lines represent the extraction efficiency for Co and Ni (Fig. 7) and the results are only valid for the range of levels of the tested variables. It is possible to observe that high Co extraction efficiencies can be obtained for any tested concentration of Cyanex 272, provided that pH is high enough, but an increase in pH (above 5) can enhance the co-

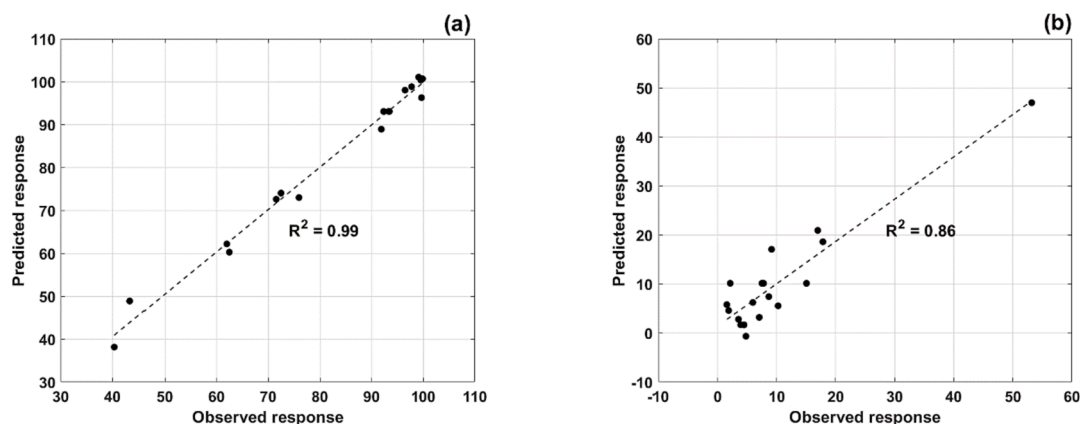


Fig. 5. Responses observed versus responses predicted by regression models for (a) Co extraction efficiency and (b) Ni extraction efficiency.

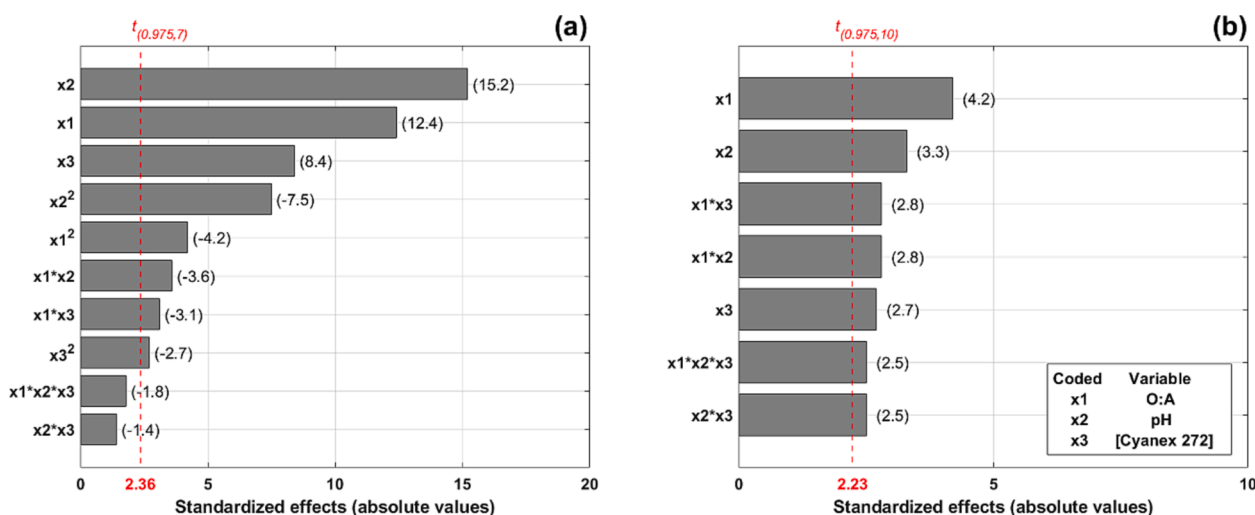


Fig. 6. Pareto charts with standardized effects of regression coefficients of regression models for (a) Co extraction efficiency and (b) Ni extraction efficiency.

extraction of Ni under certain conditions. The O:A ratio also had a positive effect on the extraction of Co and when it is ≥ 1.3 , extraction efficiencies above 60% can be reached regardless of the pH. On the other hand, lowering the O:A ratio increases the loading of the organic phase and concentrates the metal of interest, but it can also affect the viscosity and settling properties of the system as the loading increases. When comparing these conditions with those reported in the literature (Table 1), in general the extraction of Co was also in general optimal when using higher phase ratios (from 1:1) and pH (from 5). However, it is important to highlight that a comparison of the obtained results with those reported in the literature (Table 1) is not direct, considering that the process conditions and matrix vary and, the optimization in the literature was usually performed using one-variable-at-a-time.

The co-extraction of Ni remained low when using the lowest concentration of Cyanex 272 but increased to high levels when combining high pH, O:A ratio and concentration of Cyanex 272. As previously mentioned, it is expected that Mn and Cu will be fully extracted along with Co, but their concentration in the feed solution was low and for this reason, their behavior was not modelled. The extraction of Li was also not modelled and remained low in all the experiments ($<10\%$ as can be seen in Table 4). Based on these results, it is possible to conclude that high extraction efficiency of Co and limited co-extraction of Ni can be achieved under several experimental conditions, mainly by careful control of the pH. The separation factor Co/Ni was estimated based on distribution ratio for Co and Ni, which were determined based on their predicted concentrations in aqueous and organic phase. The separation

factors can be seen in Table S3 (supplementary material).

3.7. Dynamic optimization of the number of extraction stages

Optimization of the number of extraction stages needed to theoretically reach 98% Co extraction efficiency was performed in a dynamic way using the concentrations of Co and Ni in the raffinate (Table 4) as responses to fit the variables of the regression models represented in Eq. (11) and Eq. (12). The same diagnostic tests that were performed for the previous models (for efficiencies) were applied to the models for concentration and the results are presented in Figure S1, Figure S2 and Table S1.

$$Co(mg/L) = 579 - 1671x_1 - 1971x_2 - 1091x_3 + 1016x_1x_2 + 878x_1x_3 + 952x_1^2 + 1704x_2^2 + 611x_3^2 \quad (11)$$

$$Ni(mg/L) = 1790 - 210x_1 - 165x_2 - 309x_1x_2 - 308x_1x_3 \quad (12)$$

Predicted concentrations in the raffinate for several different combinations of variables were obtained using these models and the results can be observed in Table S2. These results were used to estimate the number of extraction stages needed to reach 98% extraction efficiency of Co and to estimate the co-extraction of Ni using the methodology described in section 2.6. Contour plots were constructed varying x_1 (organic to aqueous ratio) and x_2 (pH) while keeping x_3 constant (concentration of Cyanex 272). The contour plots in Fig. 8 represent the number of extraction stages needed to reach 98% extraction efficiency

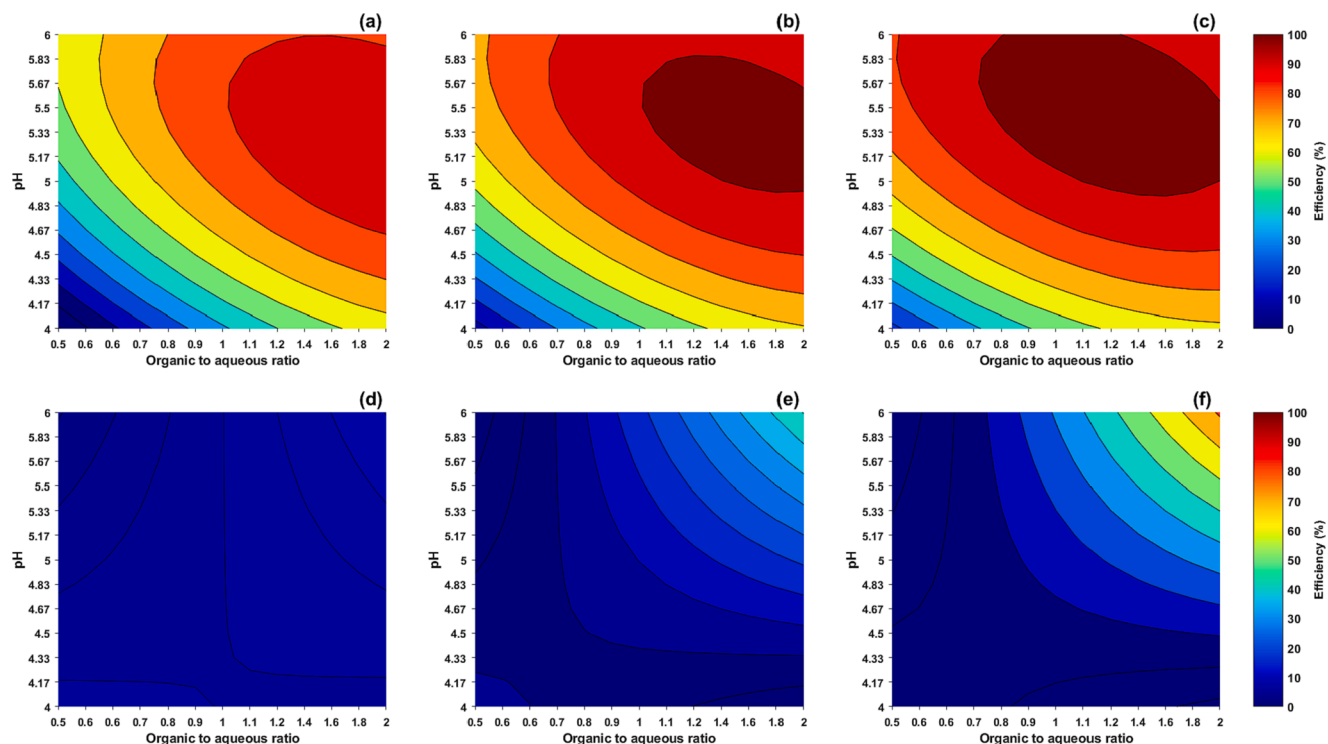


Fig. 7. Response surfaces for (a-c) Co extraction efficiency and (d-e) Ni extraction efficiency. Cyanex 272 concentrations: (a,d) 0.48 M, (b,e) 0.6 M and (c,f) 0.72 M.

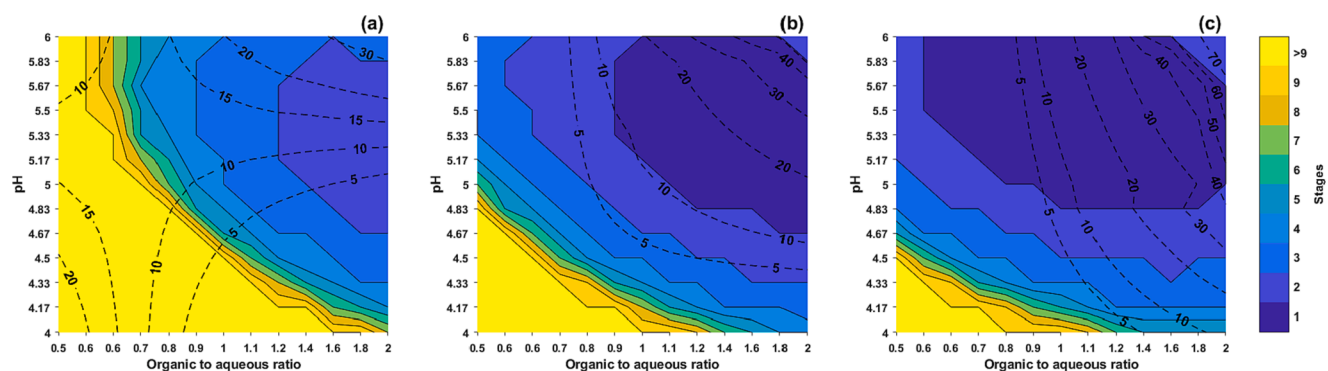


Fig. 8. Response surfaces representing the number of extraction stages estimated to be needed to reach 98% extraction efficiency of Co under different conditions. Dotted response surface representing the co-extraction of Ni. Concentrations of Cyanex 272: (a) 0.4 M, (b) 0.6 M and (c) 0.8 M.

for Co, and the dotted contour plots represent the co-extraction of Ni. The modeled results are only valid for the range of levels of the tested variables.

The number of extraction stages needed to reach 98% extraction of Co decreases with the increase in the concentration of Cyanex 272, but depending on the conditions, it also promotes an increase in the co-extraction of Ni. Although an increase in O:A ratio results in fewer extraction stages, it promotes an increase in the co-extraction of Ni as well. Thus, in general, working with lower O:A ratios seems to be more beneficial and has additional advantages regarding the pre-concentration of the loaded organic. Decreasing the pH to less than 5 will in general require more extraction stages to obtain the same desired efficiencies, especially if using low phase ratios or concentration of extractant (if the pH is 4 and the O:A 0.5:1, in general more than 9 extraction stages are required and the co-extraction of Ni is increased if the concentration of Cyanex 272 is only 0.4 M). 98% extraction of Co can be theoretically achieved in one extraction stage with co-extraction of Ni < 5% when using 0.8 M Cyanex 272, pH above 5.1 and phase ratios inferior to 0.9. These conditions lead to ~39% loading of the extractant,

which is less than the recommended limit of 60% previously discussed. If the concentration of Cyanex 272 is decreased to 0.6 M, then more extraction stages are needed (2–3) to keep the same efficiency for Co with less than 5% co-extraction of Ni. If the concentration of Cyanex 272 is decreased to 0.4 M, then it is generally necessary to increase the O:A ratio to 1.4:1–2:1 to obtain the same efficiencies with a pH ~ 5, however, at least 2 to 3 extraction stages are required. For the same conditions, if the O:A ratio is 1:1, several extraction stages (above 9) would be required to quantitatively extract Co with < 5% Ni. Based on these results, it is possible to determine that several combinations of factors allow achieving high extraction efficiency of Co (98%) with low co-extraction of Ni (<5%). Thus, this novel approach can assist the process design and optimization to decrease costs and improve resource efficiency.

4. Conclusions

Lithium-ion batteries (LiBs) are a key technology to electrify transportation and decrease our society's use of fossil fuels. Cobalt plays a central role in several LiB cathode chemistries, but it has raised concerns

regarding its supply risks. Therefore, recycling of LiBs has been considered crucial as a secondary resource to decrease Co import reliance. In this study, the recovery of Co from chloride media by solvent extraction with Cyanex 272 was optimized using the factorial design of experiments and response surface methodology. This is a relevant aspect of this work, considering that most of the available research is based on the sulfuric media, but many recycling stakeholders are interested in the hydrochloric media due to the possibility of using waste HCl in the recycling process. Thus, preliminary tests were performed to narrow the experimental conditions and the effect of different variables on the extraction efficiency of Ni and Co was investigated and optimized using the design of experiments. The extraction reached steady conditions after 10 to 15 min of contacting time and for this reason, 15 min was selected as optimal. Increasing the saponification rate promoted an increase in the extraction efficiency of different metal ions and it was set to 20%. The results indicated that Mn and Cu are in general fully co-extracted with Co at pH above 5, however, their concentration in the feed solution is low compared to Co. Lithium in general displayed low extraction efficiencies (<10%) but an increase in O:A ratio promoted an increase in the co-extraction of both Ni and Li, which is expected given the higher availability of extractant. The addition of TBP as a modifier in the preliminary studies led to a decrease in the co-extraction of Ni at high pH (5.8), but since no third phase was observed, TBP was not used in the optimization. Factorial design of experiments and response surface methodology were combined with the Kremser's Equation to estimate the number of extraction stages needed to reach 98% Co extraction efficiency under varied combinations of factors and to estimate the co-extraction of Ni. The results suggested that it is beneficial to keep the concentration of Cyanex 272 at high levels (0.6–0.8 M), the pH above 5 and the organic to aqueous ratio below 0.9:1. Under these conditions, 1 to 3 extraction stages are needed to achieve 98% extraction of Co and the co-extraction of Ni remains low (<5%). Since the number of extraction stages can affect the cost of the operation, as described by Ritcey [40] (it increases the capital costs associated with the number of tanks and inventory of solvent/extractant and operating costs associated with potentially increased losses of solvent), this proposed novel approach can be of great help in the process design and optimization. It allows determining several combinations of factors that lead to high extraction of Co and limited co-extraction of Ni and can help to improve the resource efficiency of the solvent extraction of Co from spent LiBs.

CRedit authorship contribution statement

Nathália Vieceli: Data curation, Formal analysis, Investigation, Visualization, Writing – original draft, Conceptualization, Methodology, Validation, Writing – review & editing. **Thomas Ottink:** Data curation, Formal analysis, Investigation, Visualization, Writing – original draft, Conceptualization, Methodology, Validation, Writing – original draft. **Srecko Stopic:** Resources. **Christian Dertmann:** Writing – review & editing. **Thomas Swiontek:** Writing – review & editing. **Claudia Vonderstein:** Resources. **Reiner Sojka:** Resources. **Niclas Reinhardt:** Resources. **Christian Ekberg:** Funding acquisition. **Bernd Friedrich:** Funding acquisition. **Martina Petranikova:** Conceptualization, Methodology, Validation, Writing – review & editing, Project administration, Supervision, Funding acquisition.

Declaration of Competing Interest

The authors declare that they have no known competing financial interests or personal relationships that could have appeared to influence the work reported in this paper.

Data availability

Data will be made available on request.

Acknowledgements

This research was supported by Vinnova (Grant No: 2019-02069) and by the Federal Ministry for Economic Affairs and Energy of Germany. The authors would like to acknowledge the support of Accurec Recycling GmbH (Germany) for providing samples and for valuable discussions.

Appendix A. Supplementary data

Supplementary data to this article can be found online at <https://doi.org/10.1016/j.seppur.2022.122793>.

References

- [1] H. Kawamura, M. LaFleur, K. Iversen, H.W.J. Cheng, Lithium-ion batteries: a pillar for a fossil free economy? *Front. Technol. Issues.* (2021).
- [2] International Energy Agency, Global Electric Vehicle Outlook 2022: Securing supplies for an electric future, 2022. <https://www.iea.org/reports/global-ev-outlook-2022> (accessed July 1, 2022).
- [3] Roland Berger, The Lithium-Ion (EV) battery market and supply chain - Market drivers and emerging supply chain risks, 2022. https://content.rolandberger.com/hubfs/07_presse/Roland%20Berger_The%20Lithium-ion%20Battery%20Market%20and%20Supply%20Chain_2022_final.pdf (accessed July 3, 2022).
- [4] J. Fleischmann, D. Herring, F. Liebach, M. Linder, Unlocking growth in battery cell manufacturing for electric vehicles, McKinsey & Company. (2021). <https://www.mckinsey.com/business-functions/operations/our-insights/unlocking-growth-in-battery-cell-manufacturing-for-electric-vehicles> (accessed July 4, 2022).
- [5] H.-H. Ryu, H.H. Sun, S.-T. Myung, C.S. Yoon, Y.-K. Sun, Reducing cobalt from lithium-ion batteries for the electric vehicle era, *Energy, Environ. Sci.* 14 (2021) 844–852, <https://doi.org/10.1039/D0EE03581E>.
- [6] M. Li, J. Lu, Cobalt in lithium-ion batteries, *Science* 367 (2020) (1979) 979–980, <https://doi.org/10.1126/science.aba9168>.
- [7] U.S. Department of Energy, Reducing Reliance on Cobalt for Lithium-ion Batteries, Vehicle Technologies Office. (2021). <https://www.energy.gov/eere/vehicles/articles/reducing-reliance-cobalt-lithium-ion-batteries> (accessed July 1, 2022).
- [8] E.A. Olivetti, G. Ceder, G.G. Gaustad, X. Fu, Lithium-Ion Battery Supply Chain Considerations: Analysis of Potential Bottlenecks in Critical Metals, *Joule*. 1 (2017) 229–243, <https://doi.org/10.1016/j.joule.2017.08.019>.
- [9] S.W.D. Gourley, T. Or, Z. Chen, Breaking Free from Cobalt Reliance in Lithium-Ion Batteries, *iScience*. 23 (9) (2020) 101505.
- [10] European Commission, Critical raw materials, (n.d.). https://ec.europa.eu/growth/sectors/raw-materials/areas-specific-interest/critical-raw-materials_en (accessed July 4, 2022).
- [11] K.J. Schulz, J.H. DeYoung Jr., R.R. Seal II, D.C. Bradley, Critical mineral resources of the United States—Economic and environmental geology and prospects for future supply, 2017.
- [12] X. Chen, D. Kang, L. Cao, J. Li, T. Zhou, H. Ma, Separation and recovery of valuable metals from spent lithium ion batteries: Simultaneous recovery of Li and Co in a single step, *Sep. Purif. Technol.* 210 (2019) 690–697, <https://doi.org/10.1016/j.seppur.2018.08.072>.
- [13] C. Xu, Q. Dai, L. Gaines, M. Hu, A. Tukker, B. Steubing, Future material demand for automotive lithium-based batteries, *Commun. Mater.* 1 (2020), <https://doi.org/10.1038/s43246-020-00095-x>.
- [14] M.B. Mansur, A.S. Guimarães, M. Petraniková, An Overview on the Recovery of Cobalt from End-of-life Lithium Ion Batteries, *Miner. Process. Extract. Metall. Rev.* 43 (2022) 489–509, <https://doi.org/10.1080/08827508.2021.1883014>.
- [15] C. Yang, J. Zhang, G. Liang, H. Jin, Y. Chen, C. Wang, An advanced strategy of “metallurgy before sorting” for recycling spent ternary lithium-ion batteries, *J. Clean Prod.* 361 (2022), 132268, <https://doi.org/10.1016/j.jclepro.2022.132268>.
- [16] F. Wang, R. Sun, J. Xu, Z. Chen, M. Kang, Recovery of cobalt from spent lithium ion batteries using sulphuric acid leaching followed by solid-liquid separation and solvent extraction, *RSC Adv.* 6 (88) (2016) 85303–85311.
- [17] D.S. Flett, Cobalt-Nickel Separation in Hydrometallurgy: a Review, *Chemistry for, Sustain. Develop.* 12 (2004) 81–91.
- [18] S.A. Olushola, A.A. Folahan, A.B. Alafara, J.X. Bhekumusa, S.F. Olalekan, Application of Cyanex® extractant in Cobalt/Nickel separation process by solvent extraction, *Int. J. Phys. Sci.* 8 (3) (2013) 89–97.
- [19] B. Swain, S.-S. Cho, G.H. Lee, C.G. Lee, S. Uhm, Extraction/Separation of Cobalt by Solvent Extraction: A Review, *Appl. Chem. Eng.* 26 (2015) 631–639, <https://doi.org/10.14478/ace.2015.1120>.
- [20] L. Luo, J. Wei, G. Wu, F. Toyohisa, S. Atsushi, Extraction studies of cobalt (II) and nickel (II) from chloride solution using PC88A, *Trans. Nonferrous Metals Soc. China* 16 (2006) 687–692, [https://doi.org/10.1016/S1003-6326\(06\)60122-2](https://doi.org/10.1016/S1003-6326(06)60122-2).
- [21] W.A. Rickelton, D.S. Flett, D.W. West, Cobalt-nickel separation by solvent extraction with bis(2,4,4 trimethylpentyl)phosphinic acid, *Solvent Extraction and Ion, Exchange*. 2 (1984) 815–838, <https://doi.org/10.1080/07366298408918476>.
- [22] D.S. Flett, Solvent extraction in hydrometallurgy: the role of organophosphorus extractants, *J. Organomet. Chem.* 690 (2005) 2426–2438, <https://doi.org/10.1016/j.jorganchem.2004.11.037>.

- [23] W.A. Rickelton, A.J. Robertson, J.H. Hillhouse, The significance of diluent oxidation in cobalt-nickel separation, *Solvent Extraction and Ion, Exchange*. 9 (1991) 73–84, <https://doi.org/10.1080/07366299108918043>.
- [24] J. Kang, G. Senanayake, J. Sohn, S.M. Shin, Recovery of cobalt sulfate from spent lithium ion batteries by reductive leaching and solvent extraction with Cyanex 272, *Hydrometallurgy*. 100 (2010) 168–171, <https://doi.org/10.1016/j.hydromet.2009.10.010>.
- [25] D. Quintero-Almanza, Z. Gamiño-Arroyo, L.E. Sánchez-Cadena, F.I. Gómez-Castro, A.R. Uribe-Ramírez, A.F. Aguilera-Alvarado, L.M. Ocampo Carmona, Recovery of Cobalt from Spent Lithium-Ion Mobile Phone Batteries Using Liquid-Liquid Extraction, *Batteries*. 5 (2019) 44, <https://doi.org/10.3390/batteries5020044>.
- [26] R. Torkaman, M. Asadollahzadeh, M. Torab-Mostaedi, M. Ghanadi Maragheh, Recovery of cobalt from spent lithium ion batteries by using acidic and basic extractants in solvent extraction process, *Sep. Purif. Technol.* 186 (2017) 318–325.
- [27] B. Swain, J. Jeong, J. Lee, G.-H. Lee, J.-S. Sohn, Hydrometallurgical process for recovery of cobalt from waste cathodic active material generated during manufacturing of lithium ion batteries, *J Power Sources*. 167 (2007) 536–544, <https://doi.org/10.1016/j.jpowsour.2007.02.046>.
- [28] L. Chen, X. Tang, Y. Zhang, L. Li, Z. Zeng, Y. Zhang, Process for the recovery of cobalt oxalate from spent lithium-ion batteries, *Hydrometallurgy*. 108 (2011) 80–86, <https://doi.org/10.1016/j.hydromet.2011.02.010>.
- [29] G. Dorella, M.B. Mansur, A study of the separation of cobalt from spent Li-ion battery residues, *J Power Sources*. 170 (2007) 210–215, <https://doi.org/10.1016/j.jpowsour.2007.04.025>.
- [30] V.T. Nguyen, J. Lee, J. Jeong, B.-S. Kim, B.D. Pandey, Selective recovery of cobalt, nickel and lithium from sulfate leachate of cathode scrap of Li-ion batteries using liquid-liquid extraction, *Metals Mater. Int.* 20 (2014) 357–365, <https://doi.org/10.1007/s12540-014-1016-y>.
- [31] ExxonMobil, Isopar L fluid, Product Safety Summary, (n.d.). file:///C:/Users/NathaliaVieceli/Downloads/isopar_l_fluid_product_safety_summary.pdf (accessed November 13, 2022).
- [32] ExxonMobil, Isopar L, isoparaffin fluid, sale specification, (n.d.). <https://www.exxonmobilchemical.com/en/chemicals/webapi/dps/v1/datasheets/130000000367/1/en> (accessed November 13, 2022).
- [33] D. Shi, B. Cui, L. Li, M. Xu, Y. Zhang, X. Peng, L. Zhang, F. Song, L. Ji, Removal of calcium and magnesium from lithium concentrated solution by solvent extraction method using D2EHPA, *Desalination*. 479 (2020), 114306, <https://doi.org/10.1016/j.desal.2019.114306>.
- [34] B. Kumar, A. Das, R. Alagirusamy, Compression under Static State, Elsevier, In *Science of Compression Bandages*, 2014, pp. 56–74.
- [35] N. Vieceli, F.O. Durão, C. Guimarães, C.A. Nogueira, M.F.C. Pereira, F. Margarido, Grade-Recovery Modelling and Optimization of the Froth Flotation Process of a Lepidolite Ore, *Int. J. Miner. Process* 157 (2016) 184–194, <https://doi.org/10.1016/j.minpro.2016.11.005>.
- [36] W.J. Cochran, G.M. Cox, *Experimental Designs*, John Wiley & Sons Inc, 1957.
- [37] F.M.R.C. Margarido, A Importância Da Composição Estrutural Na Lixiviação de Ligas Fe– Si, Universidade Técnica de Lisboa, Instituto Superior Técnico, 1989.
- [38] D.C. Montgomery, *Design and analysis of experiments*, 8th edition, 8th ed., John-Wiley & Sons, Inc., Hoboken, New Jersey, 2012. <https://doi.org/10.1002/ep.11743>.
- [39] N.B. Devi, K.C. Nathasarma, V. Chakravorty, Sodium salts of D2EHPA, PC-88A and Cyanex-272 and their mixtures as extractants for cobalt(II), *Hydrometallurgy*. 34 (1994) 331–342, [https://doi.org/10.1016/0304-386X\(94\)90070-1](https://doi.org/10.1016/0304-386X(94)90070-1).
- [40] G.M. Ritcey, A.W. Ashbrook, *Solvent Extraction Principles and Applications to Process Metallurgy*, Elsevier Scientific Publishing Company, New York, 1979.